



Numerical modeling of core-edge turbulent transport in realistic tokamak geometry by an advanced numerical tool

NSTX-U team meeting 14-11-2022

Manuel Scotto d'Abusco^{1,2}

¹ Aix-Marseille University-CNRS, M2P2, Ecole Centrale Marseille

² IRFM, CEA Cadarache

Introduction

- **Energy from fusion in magnetically confined devices**

- The heat and particle exhaust issues in ITER
- Investigation and prediction of the perpendicular turbulent transport

- **Numerical modeling:**

- Support and interpretation of experimental measures
- Become predictive

- **Challenges in the plasma numerical modeling:**

- Complex magnetic (X-point, close-open field lines) and wall geometries
- Multiphysics and multiscale problem: from fluid turbulence to atomic physics
- Strong anisotropy

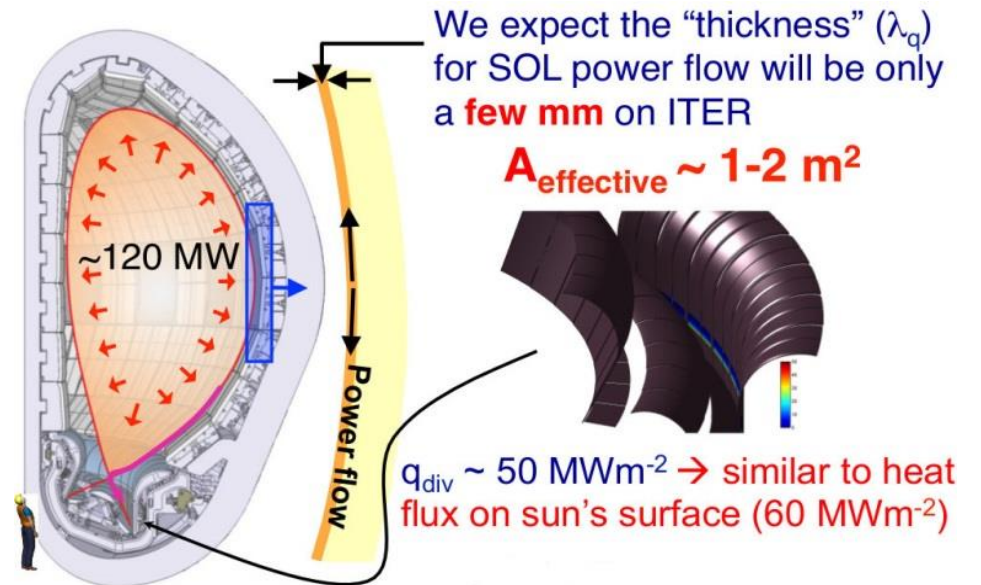
- **Different level of analysis:**

- Model Hierarchy

6D/5D kinetic/Gyrokinetic model: $\sim O(10^9)$ DoF
 $\partial_t f + v \cdot \nabla_x f + F / m \cdot \nabla_n f = C$ [Chang. Et al. PRL 2017]
 $\int_t \langle f \rangle_{cyclo} + \dots$

2D/3D Fluid model: $\sim O(10^5 - 10^7)$ DoF
 Moment distribution function + closure

Integrated: 1D model



Courtesy of A. Loarte

↑ richness of information

↓ computational cost

Current 2D/3D fluid approach: flux-aligned scheme

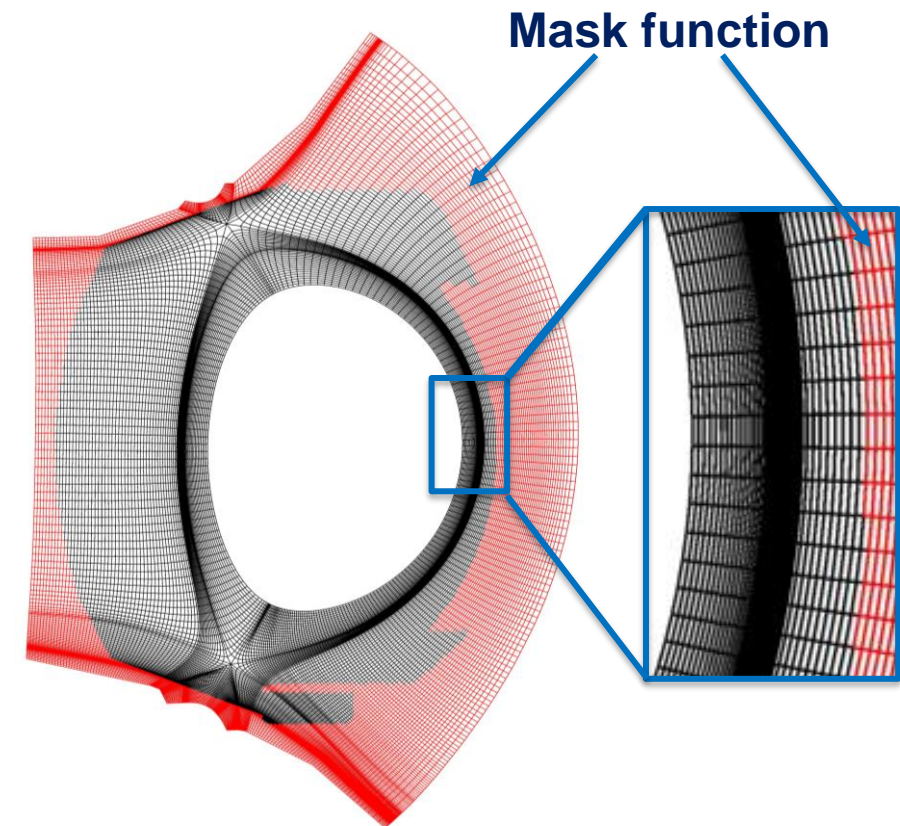
- Drift-reduced fluid model: $\lambda_c \gg \rho_L$, $\omega \ll \Omega_{c,i}$
- Current state-of-the-art averaged fluid codes based on flux aligned discretization, SE3X [H. Bufferand, NF, 2015], SOLPS-ITER [S. Wiesen et al., JNM, 2015]

Benefits

- More efficient numerically in term of DoF and implementation
- Alignment to reduce numerical diffusion induced by anisotropy

Disadvantages

- Inaccurate description of complex tokamak geometry
- Difficulty to handle singularity in the magnetic field: X point, core center
- Static magnetic equilibrium



Flux Aligned Mesh of SE3X

An original approach

- Development of an high-order finite elements method (Hybrid Discontinuous Galerkin HDG) + implicit time integration [Giorgiani *et al.* J. Comp. Phys. 2018] in the SOLEDGE3X suite of codes

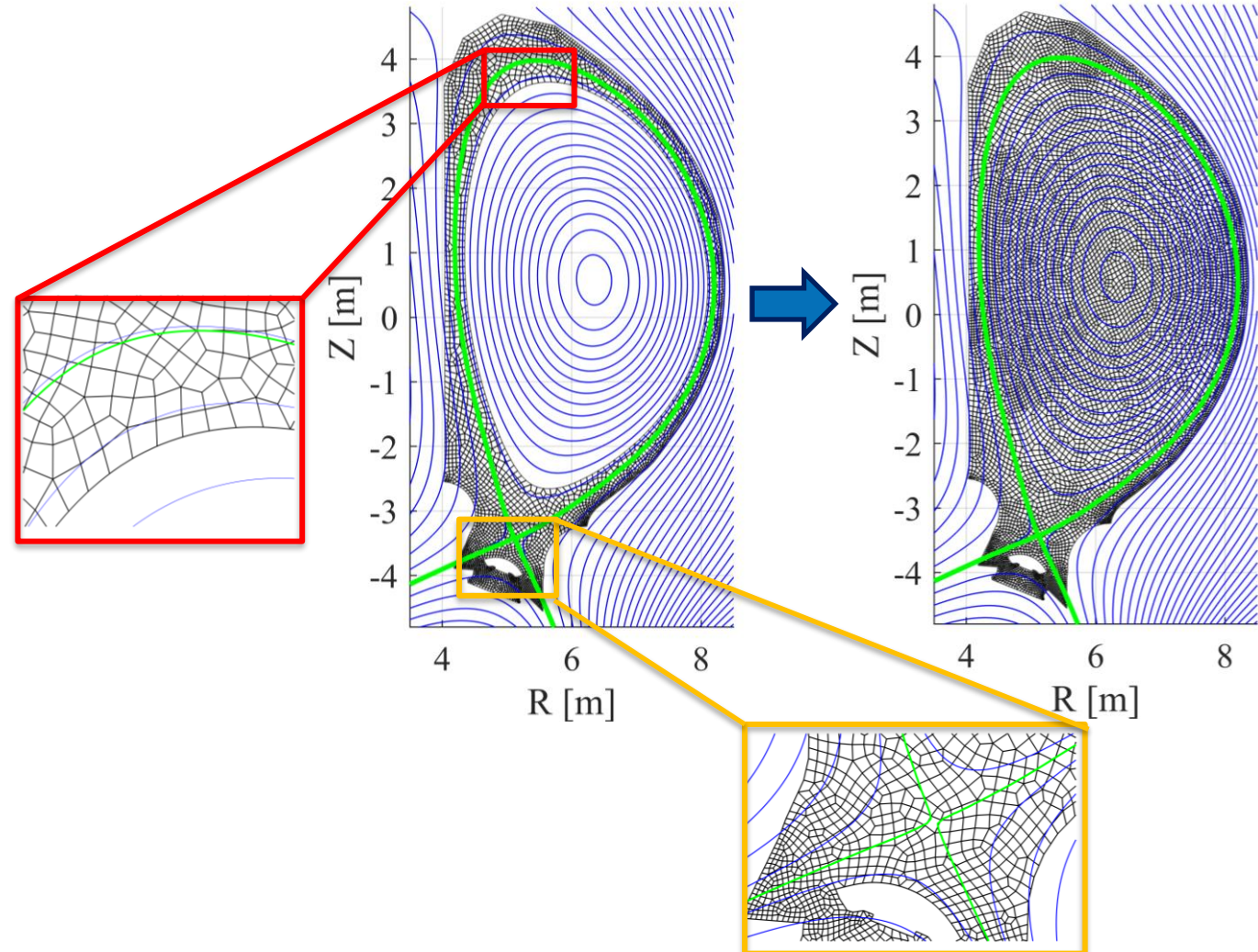
→ MPI-OMP SOLEDGE3X-HDG
[Giorgiani *et al.* Comp. Phys. Com. 2020]

→ Non-aligned discretization: unstructured meshes

- Accurate description of PFCs
- Full tokamak cross section
- Magnetic equilibrium free

→ High-order
• Reduced DoF

→ Full implicit time
• Long time integration for full experimental discharges



Outlines

- **Mathematical and numerical model**
- Verification and validation
- Core-edge coupling and sources
- Preliminary investigation of a detached plasma
- Full 2D transport simulations of an entire experimental discharge
- Steady vs transient

The mathematical model

- Braginskii 2D fluid reduced model [Braginskii 1965]

$$\left\{ \begin{array}{l} \partial_t n + \nabla \cdot (n u \mathbf{b}) - \nabla \cdot (D \nabla_{\perp} n) = S_n \\ \partial_t (m_i n u) + \nabla \cdot (m_i n u^2 \mathbf{b}) + \nabla_{\parallel} (k_b n (T_e + T_i)) - \nabla \cdot (\mu \nabla_{\perp} (m_i n u)) = S_{\Gamma} \\ \partial_t \left(\frac{3}{2} k_b n T_i + \frac{1}{2} m_i n u^2 \right) + \nabla \cdot \left(\left(\frac{5}{2} k_b n T_i + \frac{1}{2} m_i n u^2 \right) u \mathbf{b} \right) - n u e E_{\parallel} - \nabla \cdot \left(\frac{3}{2} k_b (T_i D \nabla_{\perp} n + n \chi_i \nabla_{\perp} T_i) \right) \\ - \nabla \cdot \left(-\frac{1}{2} m_i u^2 D \nabla_{\perp} n + \frac{1}{2} m_i \mu n \nabla_{\perp} u^2 \right) - \nabla \cdot (k_{\parallel i} T_i^{\frac{5}{2}} \nabla_{\parallel} T_i \mathbf{b}) + \frac{3}{2} \frac{k_b n}{\tau_{ie}} (T_e - T_i) = S_{E_i} \\ \partial_t \left(\frac{3}{2} k_b n T_e \right) + \nabla \cdot \left(\frac{5}{2} k_b n T_e u \mathbf{b} \right) + n u e E_{\parallel} - \nabla \cdot \left(\frac{3}{2} k_b (T_e D \nabla_{\perp} n + n \chi_e \nabla_{\perp} T_e) \right) - \nabla \cdot (k_{\parallel e} T_e^{\frac{5}{2}} \nabla_{\parallel} T_e \mathbf{b}) \\ - \frac{3}{2} \frac{k_b n}{\tau_{ie}} (T_e - T_i) = S_{E_e} \end{array} \right. \quad (1)$$

where $\nabla_{\parallel} = \mathbf{b} \cdot \nabla$, $\nabla_{\perp} = \nabla - \mathbf{b} \nabla_{\parallel}$, and $\mathbf{b} = \frac{\mathbf{B}}{\|\mathbf{B}\|}$. D , μ , χ_i , χ_e perpendicular diffusion coefficients and $k_{\parallel i}$, $k_{\parallel e}$ parallel heat fluxes diffusion coefficient;

- Plasma-wall interactions prescribed by the Bohm boundary condition:

→ Outgoing supersonic velocity

$$u \geq c_s \quad \text{if } \mathbf{b} \cdot \mathbf{n} > 0$$

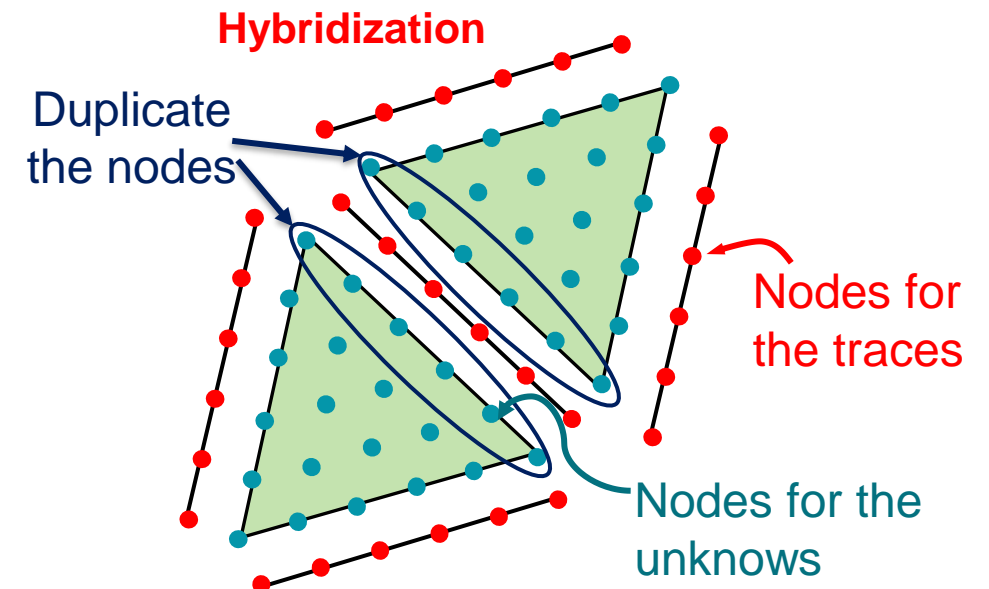
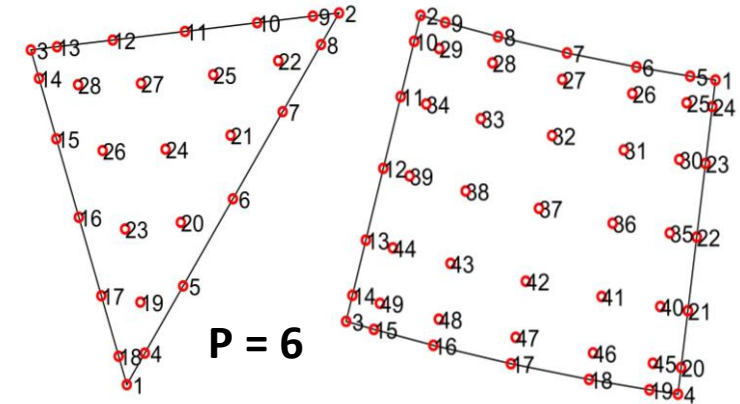
→ Parallel heat fluxes imposed to the sheath transmission values

$$u \leq -c_s \quad \text{if } \mathbf{b} \cdot \mathbf{n} < 0$$

The HDG method

HDG:HIGH ORDER finite element method based on **HYBRID DISCONTINUOUS** Galerkin [G.Giorgiani,J.C.Physics,2018]

- **High Order:** the solution is approximated by an high-order polynomial in each element
- **Discontinuous:**
 - Resolution of local problem posed in weak form;
 - Duplication of the nodes at the element borders;
 - Global problem derived by weakly imposing the continuity of numerical fluxes across the borders;
- **Hybrid:** introduction of new unknowns, called trace solutions, defined on the element border. Reduction of DOF.



The HDG formulation: local problem

- Local problem in each element for the conservative variables $U, Q = \nabla U$

$$U = \begin{Bmatrix} U_1 \\ U_2 \\ U_3 \\ U_4 \end{Bmatrix}, = \begin{Bmatrix} n \\ nu \\ nE_i \\ nE_e \end{Bmatrix} \quad Q = \nabla U = \begin{bmatrix} \nabla U_1^T \\ \nabla U_2^T \\ \nabla U_3^T \\ \nabla U_4^T \end{bmatrix} = \begin{bmatrix} U_{1,x} & U_{1,y} \\ U_{2,x} & U_{2,y} \\ U_{3,x} & U_{3,y} \\ U_{4,x} & U_{4,y} \end{bmatrix} = \begin{bmatrix} Q_{11} & Q_{12} \\ Q_{21} & Q_{22} \\ Q_{31} & Q_{32} \\ Q_{41} & Q_{42} \end{bmatrix}$$

$$\begin{cases} Q - \nabla U = 0 & \text{in } \Omega_i \times]0, T_f[\\ \partial_t U + \nabla \cdot (\mathbf{F} - D_f Q + D_f Q \mathbf{b} \otimes \mathbf{b} - \mathbf{F}_t) + \mathbf{f}_{E_{||}} + \mathbf{f}_{EX} - \mathbf{g} = \mathbf{s} & \text{in } \Omega_i \times]0, T_f[\\ U(\mathbf{x}, t) = \hat{U}(\mathbf{x}, t) & \text{in } \partial\Omega_i \times]0, T_f[\\ U(\mathbf{x}, 0) = U_0 & \text{in } \Omega_i \end{cases} \quad (2)$$

convection+diffusion
(isotropic part)

diffusion
(anisotropic part)

Parallel Diffusion

→ a elemental solution for the vector U, Q is recovered in each element in function of the trace unknown \hat{U}

The HDG formulation: global problem

- \hat{U} is the actual unknown of the problem determined by setting up the following global problem:

$$\left\langle \hat{\mathbf{v}}, (\mathbf{F} - D_f \mathbf{Q} + D_f \mathbf{Q} \mathbf{b} \otimes \mathbf{b} - \mathbf{F}_t) \mathbf{n} + \boldsymbol{\tau} (\mathbf{U} - \hat{\mathbf{U}}) \right\rangle_{\mathcal{T} \setminus \partial\Omega} + \left\langle \hat{\mathbf{v}}, \mathbf{B}_{BC} \right\rangle_{\partial\Omega} = 0 \quad (4)$$

→ $\mathcal{T} = \bigcup_{i=1}^{N_{el}} \partial\Omega_i$ mesh skeleton

→ \mathbf{B}_{BC} is a flux vector which defines the boundary condition on $\partial\Omega$

- \mathbf{U} and \mathbf{Q} solution of the local problem Eqs. (3) in function of $\hat{\mathbf{U}}$

- **Hybridization**

- Eq. (4) weakly imposes the normal fluxes at the element boundary and it depends only by the unknown $\hat{\mathbf{U}}$
- reduce the size of the linear system generated by the element discretization

Outlines

- **Mathematical and numerical model**
- **Verification and validation**
- Core-edge coupling and sources
- Preliminary investigation of a detached plasma
- Full 2D transport simulations of an entire experimental discharge
- Steady vs transient

Verification of the code

- **MMS** : code verification in realistic tokamak geometry \rightarrow entire 2D cross section
 - \rightarrow scan in the order of the polynomial of interpolation $p = 1, \dots, 4$
 - \rightarrow scan in the characteristic length h of each element $h = 1/2^m$ for $m = 1, \dots, 5$
- Analytical solution \mathbf{U}_a considered for all the variables

$$n = 2 + \sin(2\pi x)\sin(2\pi y) \quad u = \cos(2\pi x)\cos(2\pi y)$$

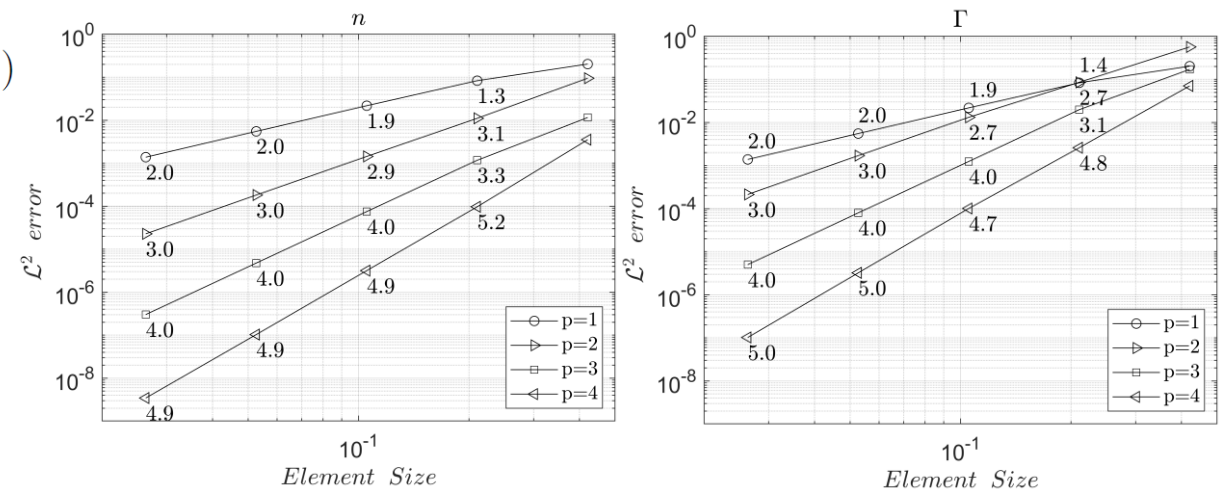
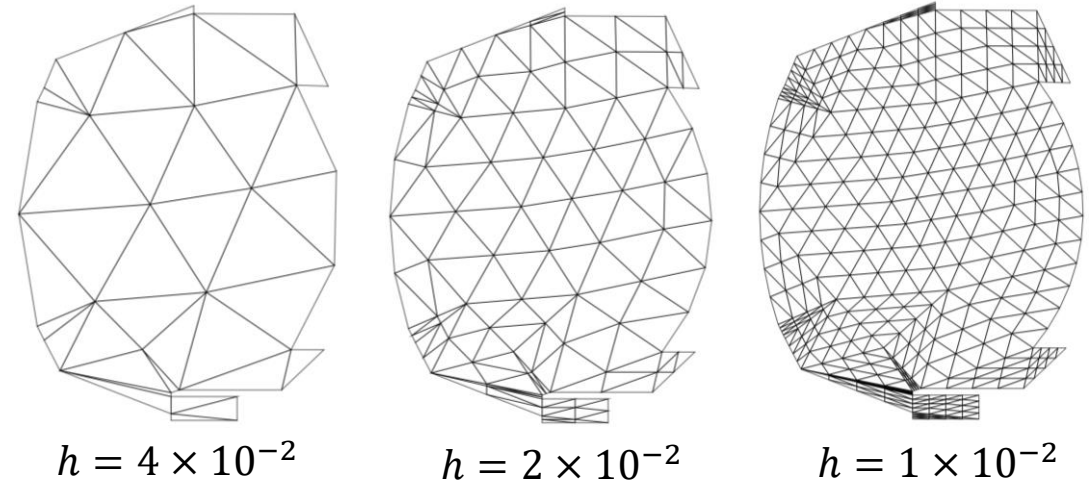
$$E_i = 20 + \cos(2\pi x)\sin(2\pi y) \quad E_e = 10 - \sin(2\pi x)\cos(2\pi y)$$

- Cartesian magnetic field + Dirichlet BC

$$b_x = \frac{1}{30}(x - y^2 + 2) \quad b_y = \frac{1}{30}(xy + y)$$

- \mathcal{L}^2 error defined as the distance between the numerical solution \mathbf{U} and the exact solution of the modified problem \mathbf{U}_a

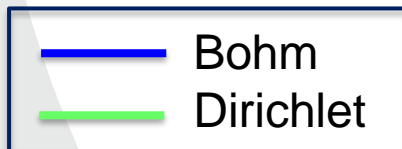
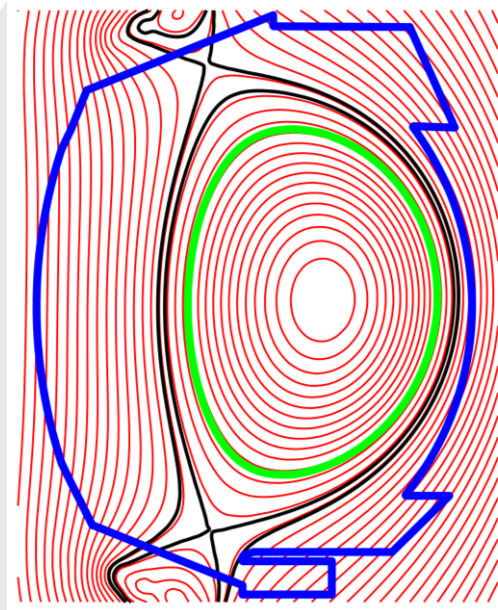
$$\mathcal{L}^2 = \sqrt{\int_{\Omega} (\mathbf{U} - \mathbf{U}_a)^2}$$



\rightarrow recovered the expected theoretical rate of convergence $p+1$

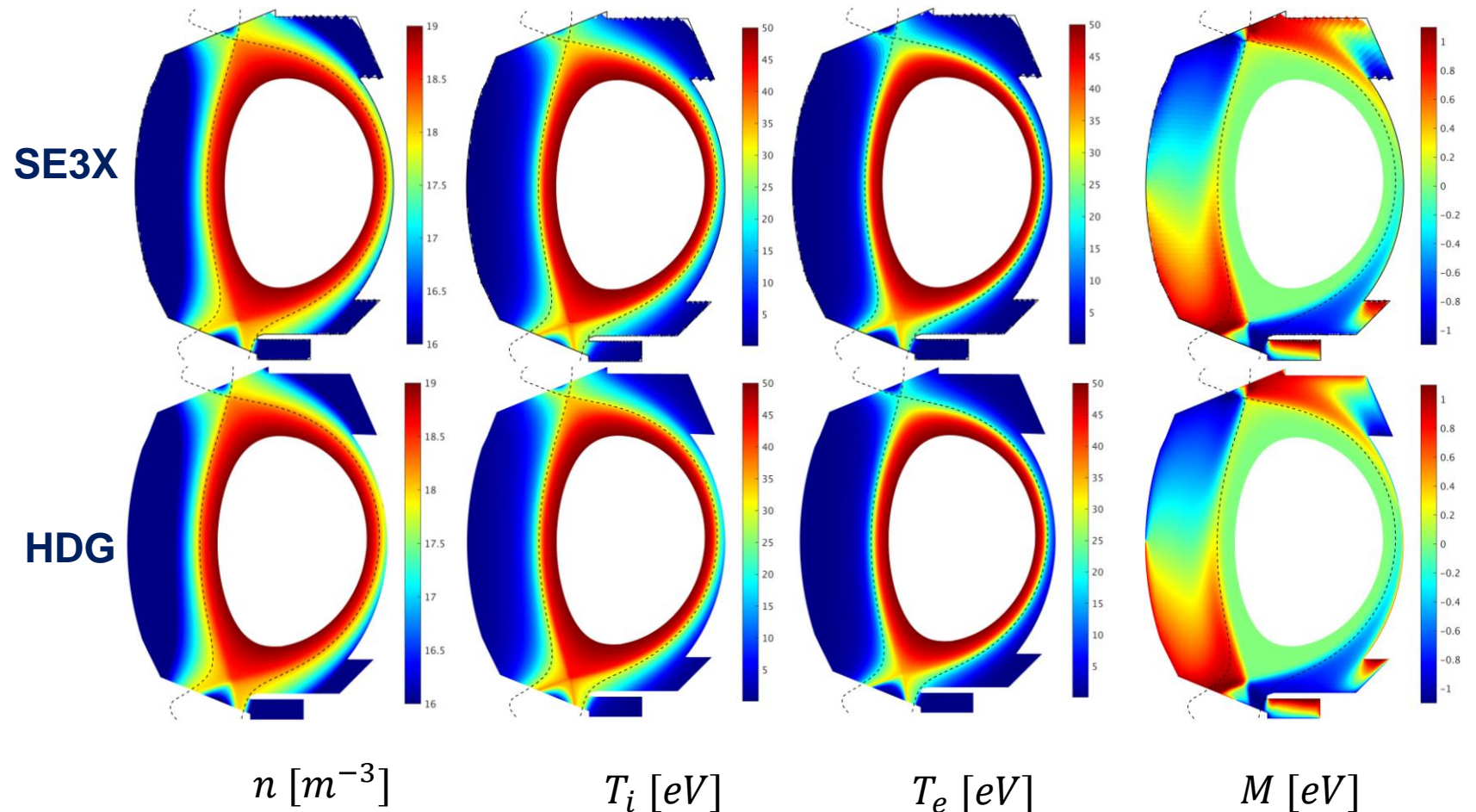
Benchmarking with SE3X (1/2)

- Comparison with the well established code SE3X in WEST geometry [H. Bufferand, NF, 2015]

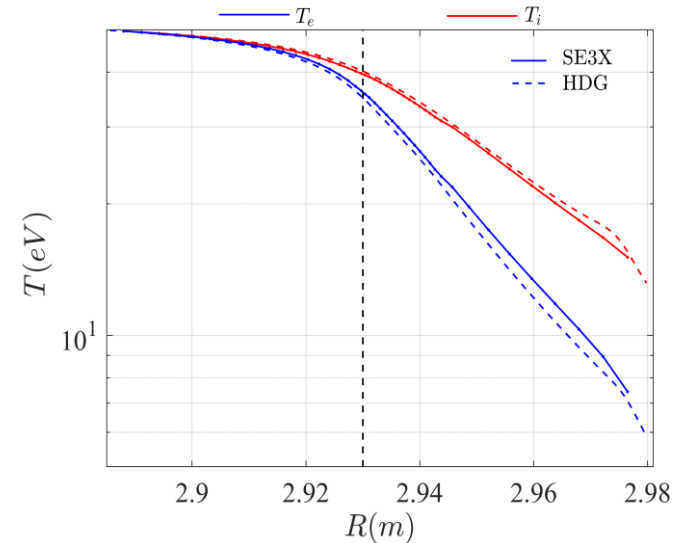
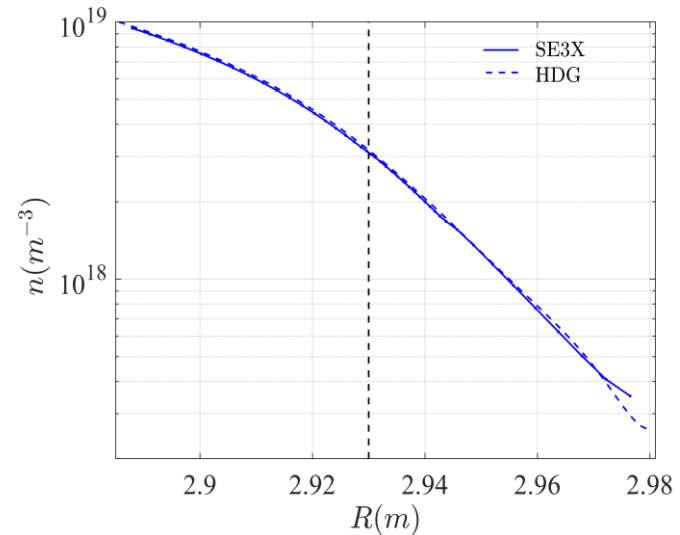
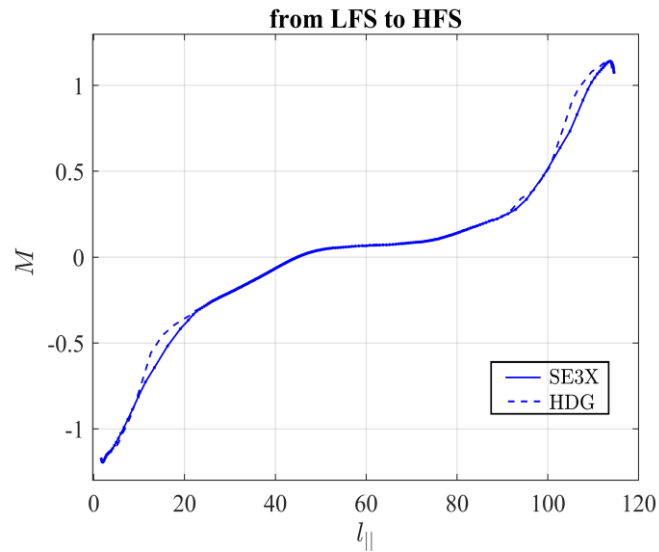


- $n_{Dir} = 1e19 [m^{-3}]$
- $u_{Dir} = 0 [m/s]$
- $T_{i,Dir} = T_{e,Dir} = 50 [eV]$

$$D = \mu = \chi_i = \chi_e = 1 \frac{m^2}{s}$$



Benchmarking with SE3X(2/2)



- Good agreement in between SE3X and SE3X-HDG profiles
- Small discrepancy in the far SOL especially in ion and electron mid-plane profiles
 - geometry discretization
 - different numerical method: Finite Volume for SE-3X vs Finite Element for SE-HDG
 - time of computation: 40 m SE3X-HDG, 12-14h SE3X

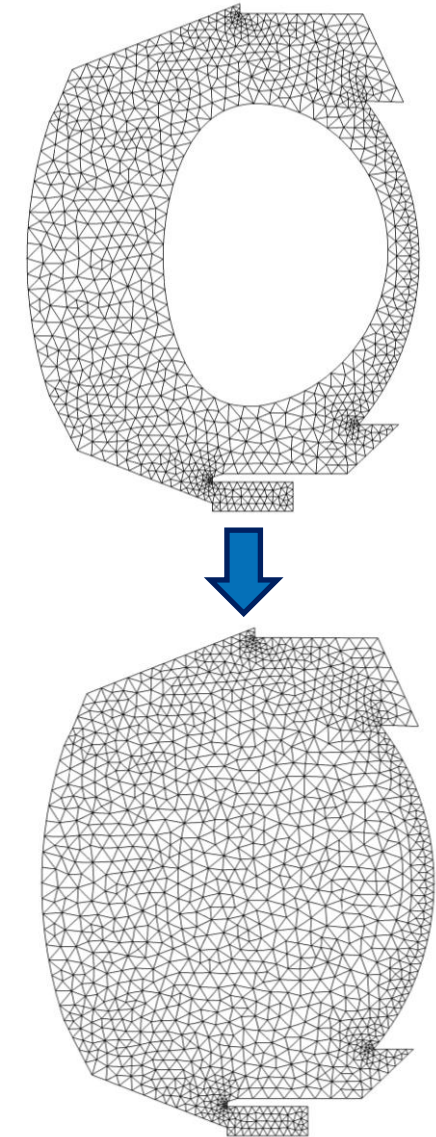
The benchmark test is satisfying making us confident on the non-aligned approach !!

Outlines

- Mathematical and numerical model
- Verification and validation
- **Core-edge coupling and sources**
- Preliminary investigation of a detached plasma
- Full 2D transport simulations of an entire experimental discharge
- Steady vs transient

Core-edge coupling and sources

- Enrich core physics allowing to study
 - Plasma heating
 - Energy redistribution
 - Transport of impurity
 - Full experimental discharge simulation with variable magnetic equilibrium
- Source location is a critical point in plasma simulation
[D. Galassi, PoP, 2022]
 - Remove and replace the badly posed Dirichlet/ Neumann BC
 - Extension of the domain of computation up to the core
 - Investigation of the entire tokamak cross-section
- Need sources to get a stationary state in the whole domain
 - Development of self-consistent sources of particle and energy
 - **Source of particle:** Neutral Model
 - **Source of energy:** Ohmic Heating



Neutral model

- Crucial role due to strong interaction with plasma
- Kinetic approach + Monte-Carlo solver: **EIRENE** [D. Reiter et al., FSaT, 2005]
 - Rich and accurate in term of physics
 - Slow convergence in high collisional regime
- Diffusive fluid neutral + plasma recycling at wall (charge exchange dominated regimes) [Horsten et al., NF, 2017]

$$\begin{aligned} \partial_t n_n - \nabla \cdot (D_{n_n} \nabla n_n) &= S_{n_n,iz} + S_{n_n,rec} + S_{n_n} \\ - D_{n_n} \nabla n_n \cdot \mathbf{n} &= -R(-D_{n_n} \nabla n \cdot \mathbf{n} + n u \mathbf{b} \cdot \mathbf{n}) \end{aligned}$$

→ coupled to plasma with ionization-recombination-radiation terms $S_{n,iz}, S_{n,rec}, S_{\Gamma,cx}, S_{\Gamma,rec}, S_{E_i,iz}, S_{E_i,cx}, S_{E_i,rec}, S_{E_e,iz}, S_{E_e,rec}$: linear system for 5 Eqs. (4 for plasma + 1 for neutrals)

- **Source of particle** to fill up the core region
 - Easily implementable in the HDG framework
 - Allows to compute fast steady state solution (2h-6h in WEST geometry)
 - More realistic description of plasma behaviour close to the target

Ohmic source

- Ohmic source of power given by

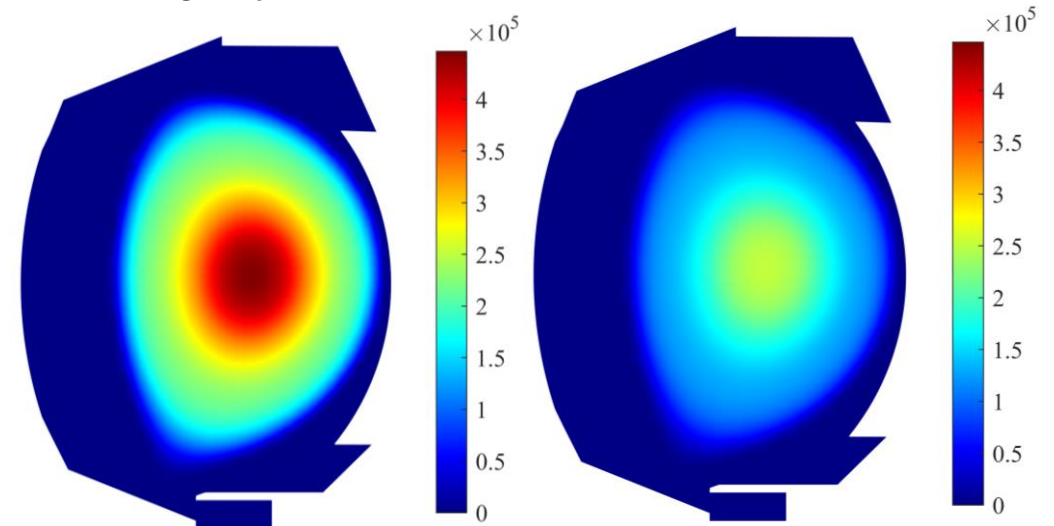
$$S_{Ohmic} = \eta j^2 = 0.51 \frac{m_e^{1/2} e^2 \ln \Lambda}{3(2\pi)^{3/2} \epsilon_0^2} \frac{1}{T_e^{3/2}} j^2$$

Spitzer Harm resistivity

- Current density 2D distribution from equilibrium experimental reconstruction
- Non linear coupling with plasma temperature

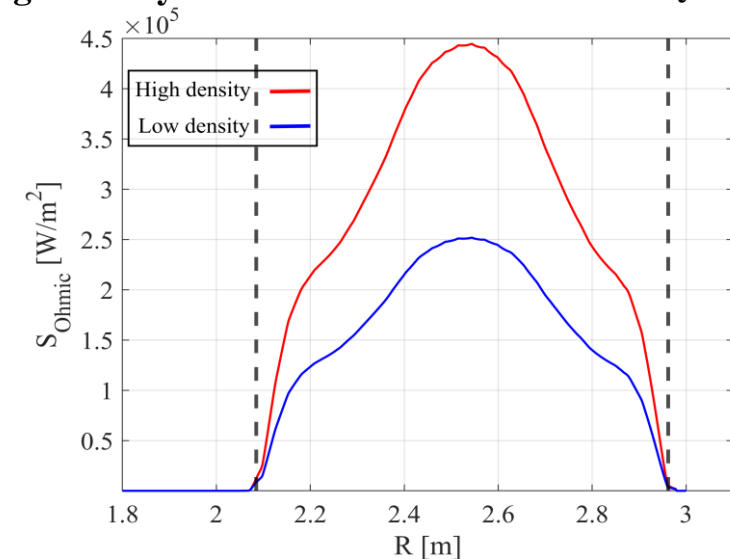
- Easily implementable for other sources:
 - RF, ICRH, ECRH, LH ...

S_{Ohmic} [W/m³] Shot #54487 t = 4.5 [s]



High density

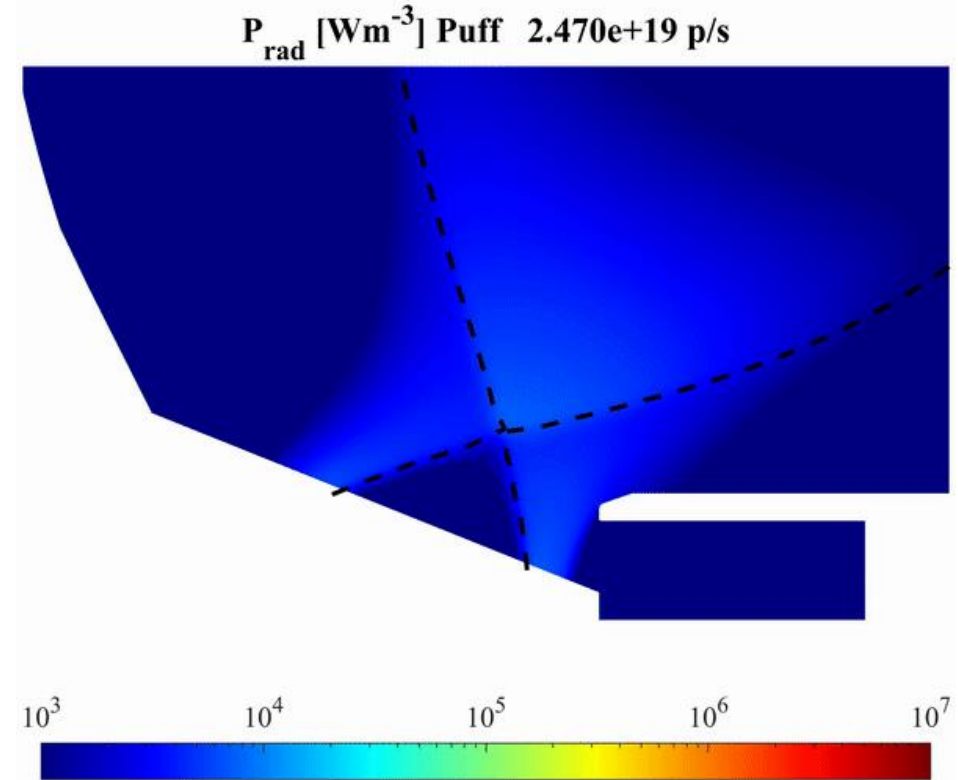
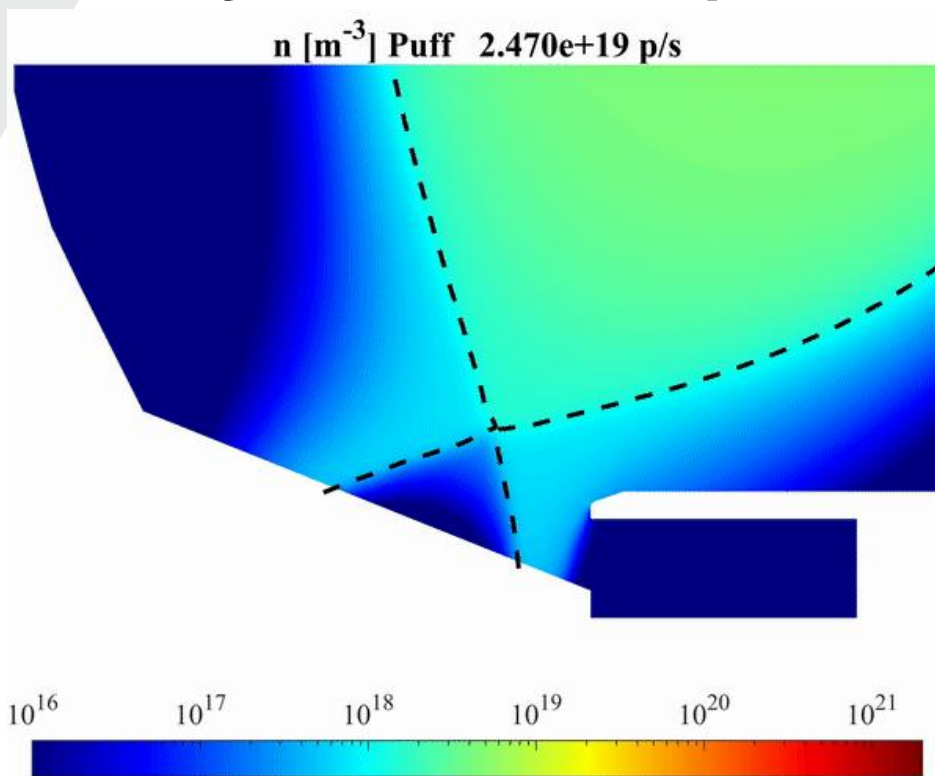
Low density



Outlines

- Mathematical and numerical model
- Verification and validation
- Core-edge coupling and sources
- **Preliminary investigation of a detached plasma**
- Full 2D transport simulations of an entire experimental discharge
- Steady vs transient

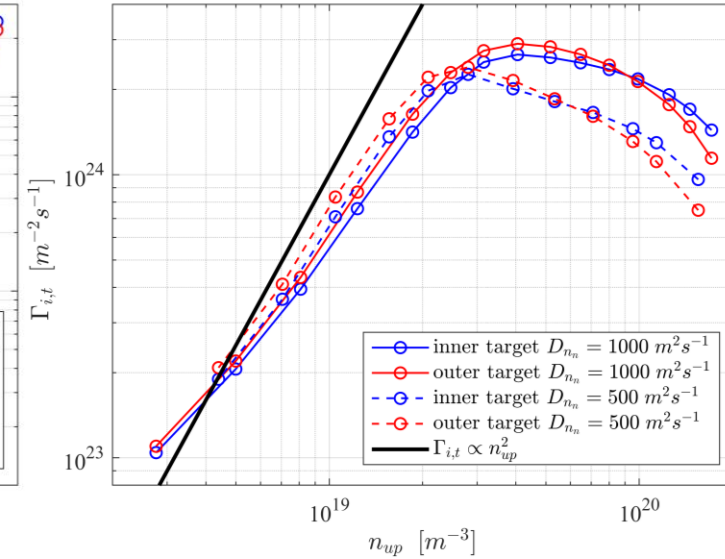
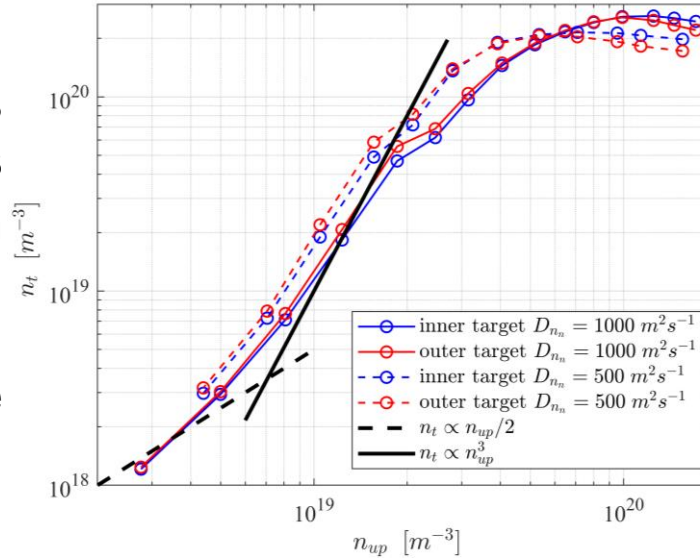
Density scan toward plasma detachment



- Analysis of plasma detachment achievement
 - Double single null magnetic configuration as in benchmark test with SE3X
 - $D = \mu = \chi_i = \chi_e = 1 \text{ m}^2/s$
 - Ohmic source of power in the core
 - Neutral model + plasma recycling with $R = 0.99$
 - Prescribed puff with $D_{nn} = 1000 \text{ m}^2/s$.

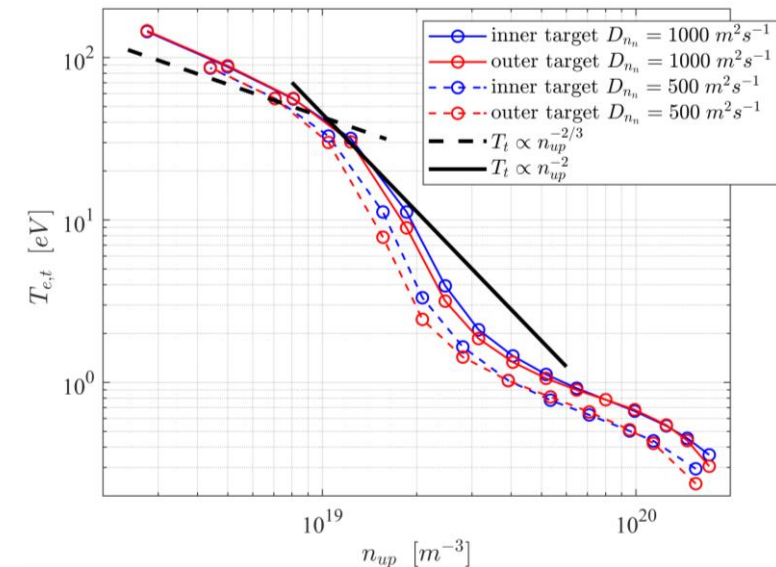
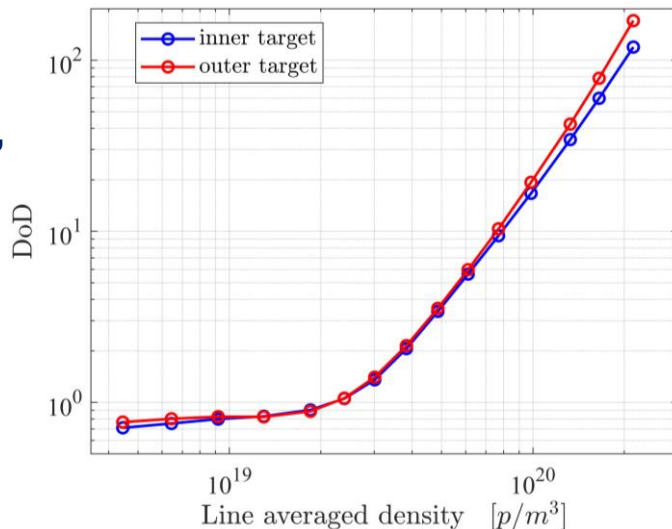
Analysis with the 2 point model (2PM)

- Clear evidences of plasma detachment
 - Comparison with 2PM predicted slopes for $n_t, \Gamma_t, T_{e,t}$ in function of n_{up} indicates a transition from sheath limited to high recycling regime
 - Saturation and decrease of n_t
 - Rollover of the flux of particle at the target contrary to 2PM which prescribes



$$\Gamma_t = n_t c_s = \left(\frac{7\gamma L_c}{8k_0 m_i} \right)^2 \frac{n_{up}^2}{T_{up}^{3/2}}$$

→ DoD ≥ 2
[A. Loarte, et al.,
NF, 1998]

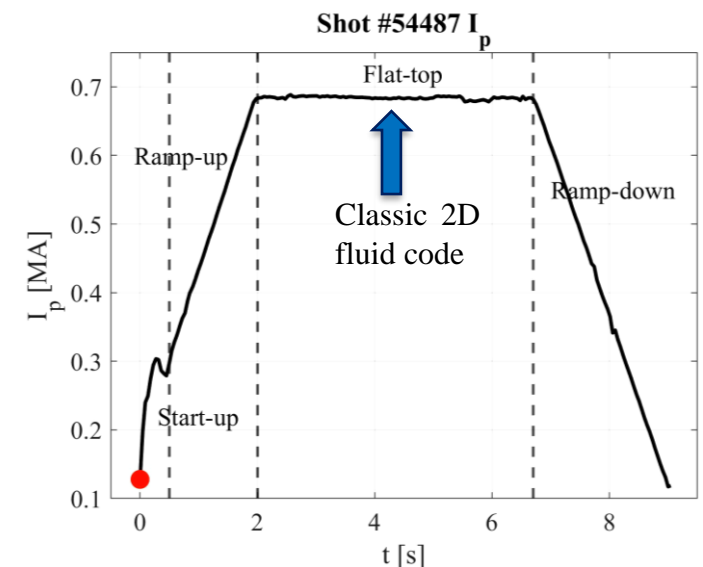
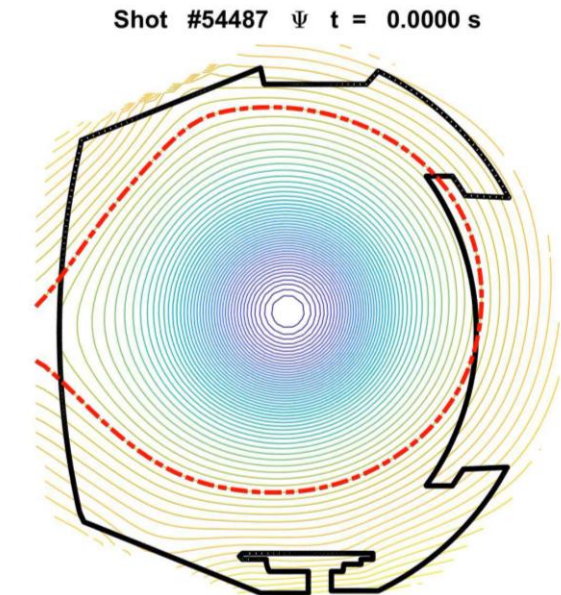


Outlines

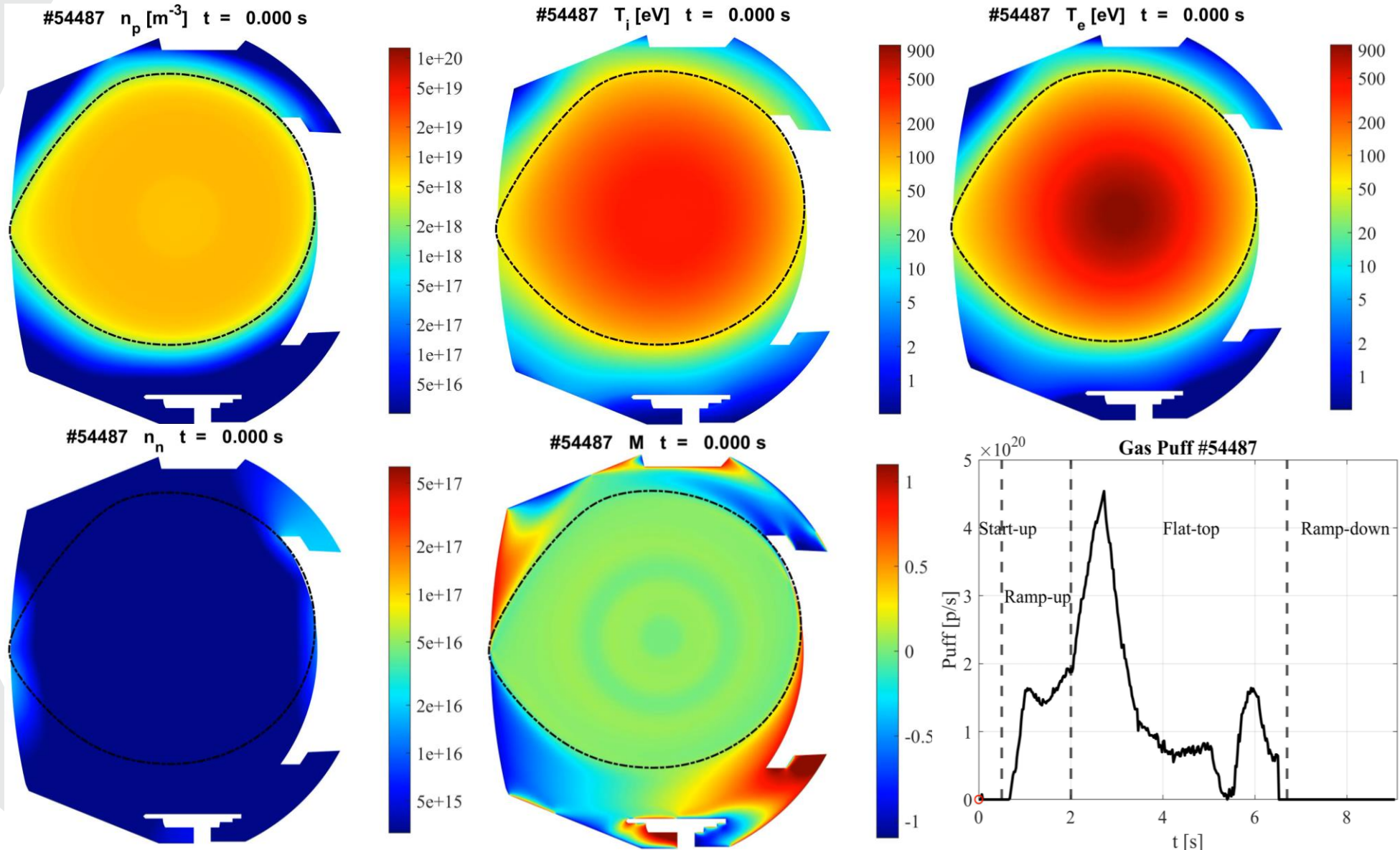
- Mathematical and numerical model
- Verification and validation
- Core-edge coupling and sources
- Preliminary investigation of a detached plasma
- **Full 2D transport simulations of an entire experimental discharge**
- Steady vs transient

Full WEST discharge: shot #54487

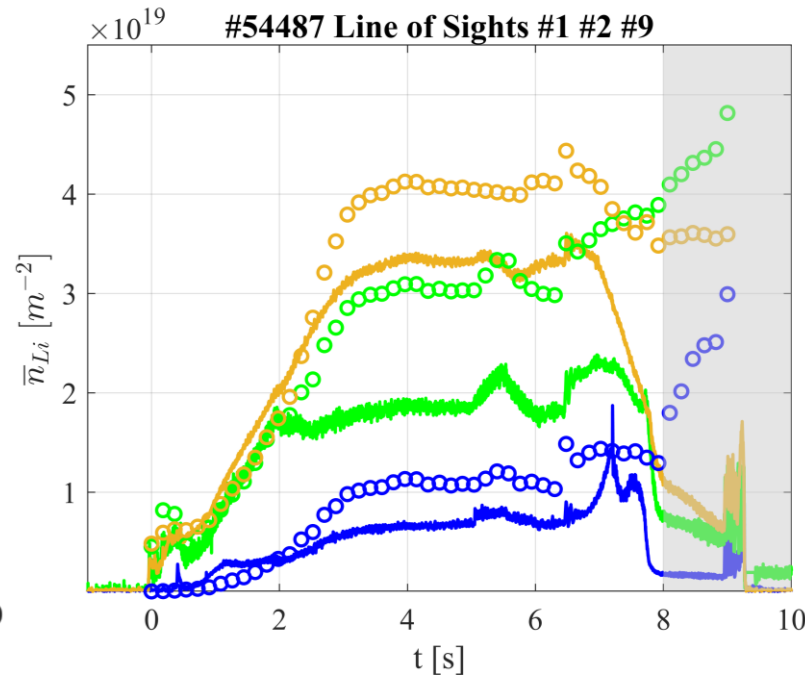
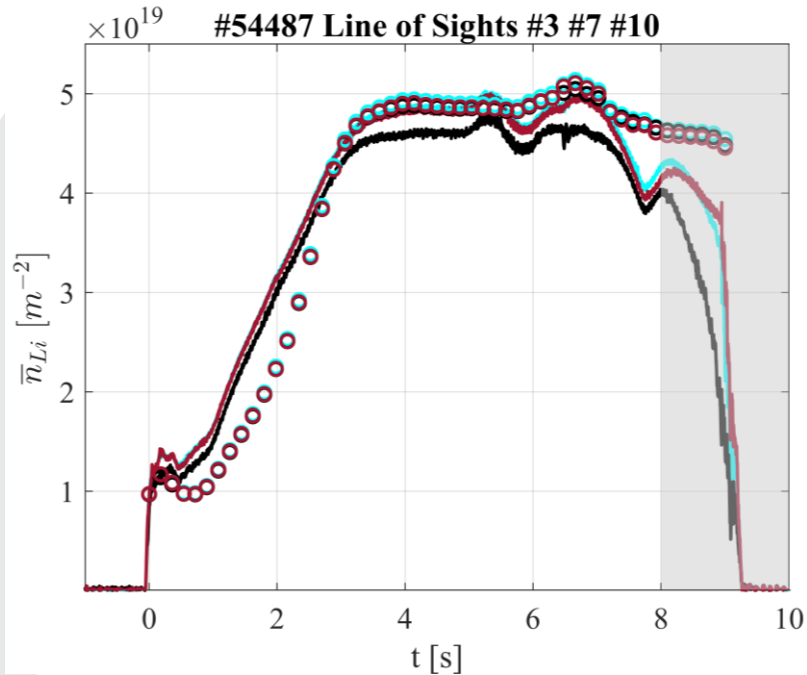
- 2D transport simulation of an entire experimental discharge
 - impact of the transient phase: limiter-divertor(L-D)
 - comparison with experimental data
 - analysis of fluxes at the PFCs
 - impurity contamination (W)
- Magnetic equilibrium and current 2D distribution from experimental reconstruction
 - WEST shot #54487 (pure Ohmic discharge)
- Numerical and physical parameters
 - $D = \mu = \chi_i = \chi_e = 0.5 \text{ m}^2/\text{s}$ $D_{nn} = 2000 \text{ m}^2/\text{s}$
 - $dt = 0.02 \text{ s}$
 - $R = 0.998 + \text{experimental puff rate}$
 - 403 different equilibriums for a total time of integration of 10 s
 - Real time of computation: 240 h, 1 node 32 cpus, OMP



WEST Shot #54487: 2D map of the fluid quantities



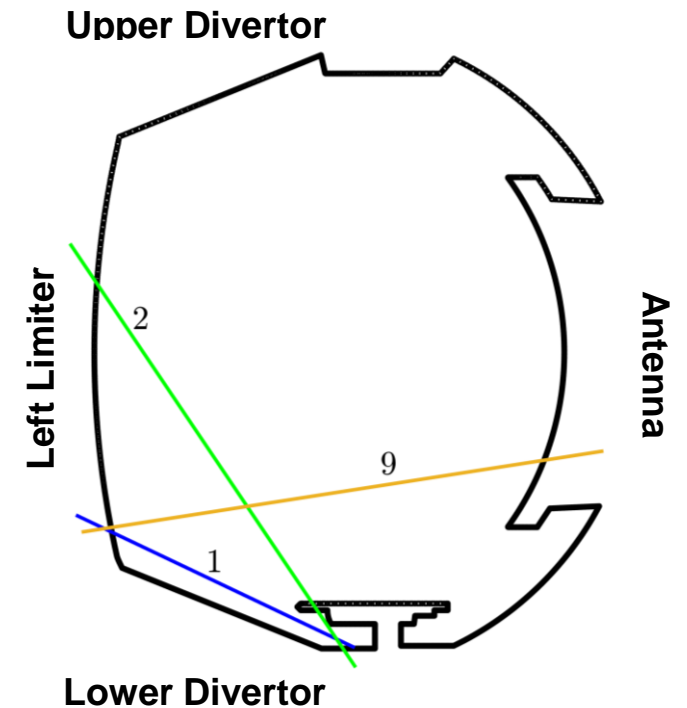
WEST Shot #54487: comparison with experiments



[MS d'Abusco et al. N. Fus. 2022]

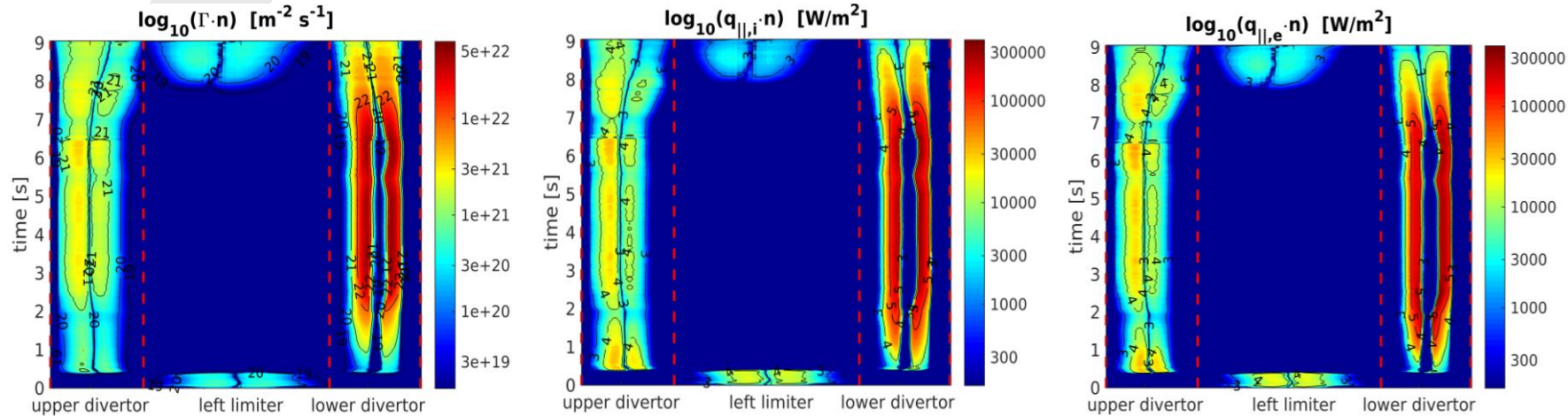
● Interferometry data analysis:

- Qualitatively agreement with experimental data (ram-up, flat-top)
- Good reproduction of central line integrated density (LoS 3,7,10)
- Imperfect agreement with line integrated density close to X-point (LoS 1, 2, 9)
- Inability to reproduce the last second of the discharge (8-9 s MHD events, instabilities ecc ...)



WEST Shot #54487: quantities at PFCs vs Time (1/2)

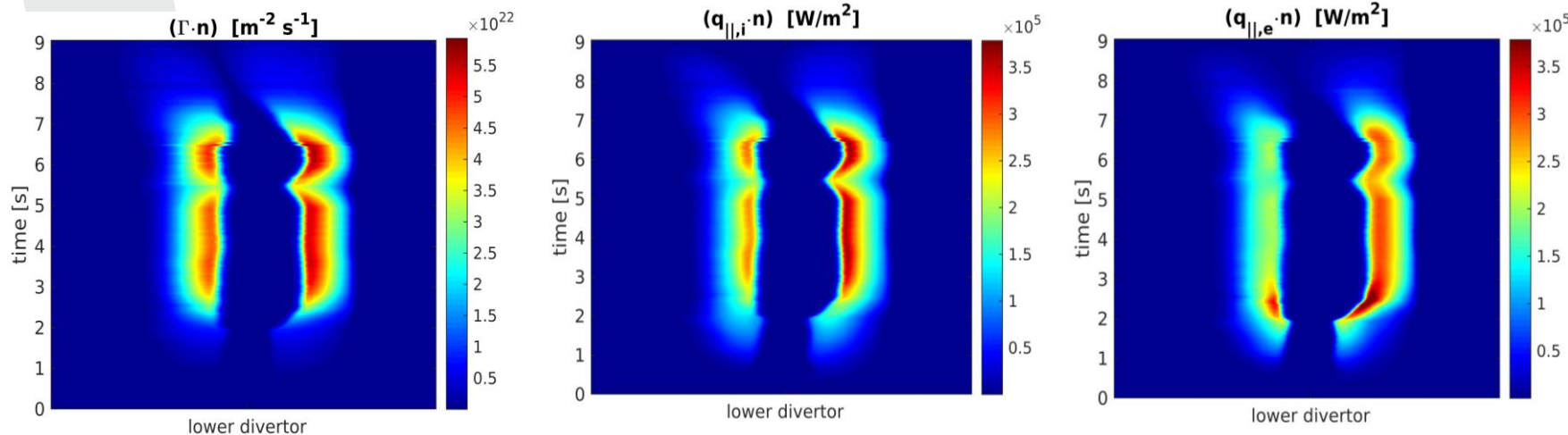
- $\Gamma, q_{\parallel,i}, q_{\parallel,e}$ in function of wall coordinates (Log Scale):



→ Fluxes cocentrated on the HFS limiter for $t < 1$ s

→ Peaks reached at the L. Div. with maximum located at the outer target (LFS)

- $\Gamma, q_{\parallel,i}, q_{\parallel,e}$ at lower divertor (Linear Scale):

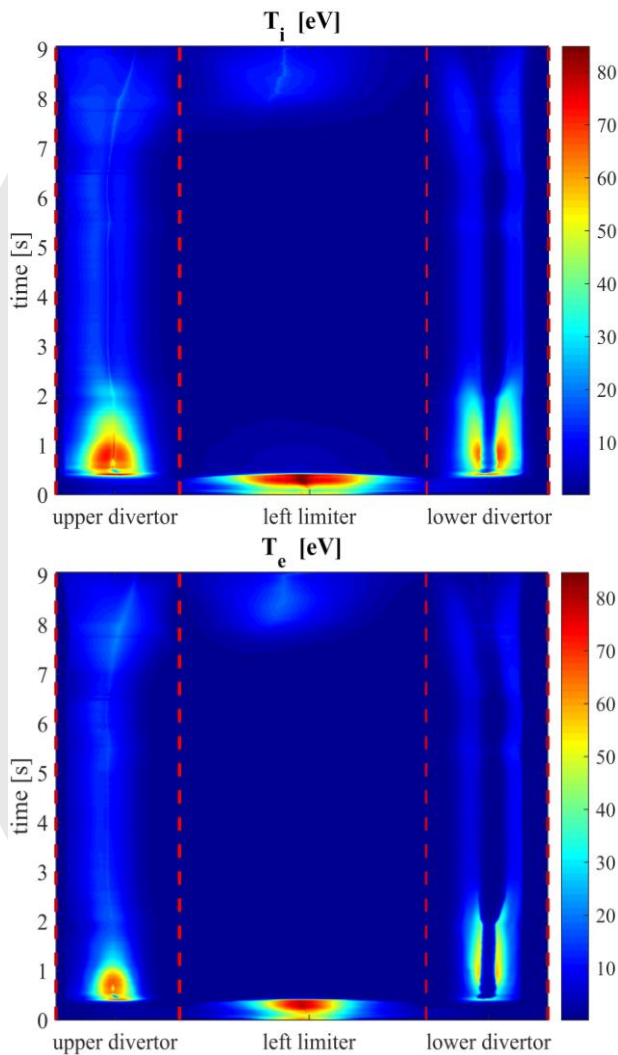


→ $(q_{\parallel,i} \cdot n) > (q_{\parallel,e} \cdot n)$ in the stationary phase contrary to transient phase

→ Location of the peaks spreads in time along L. Div. coordinates

[MS d'Abusco *et al.* N. Fus. 2022]

WEST Shot #54487: quantities at PFCs vs Time (2/2)



Temperatures 2D map:

→ erosion Map

$$\propto \Gamma \cdot n Y(T_{i,e}, Z_{eff})$$

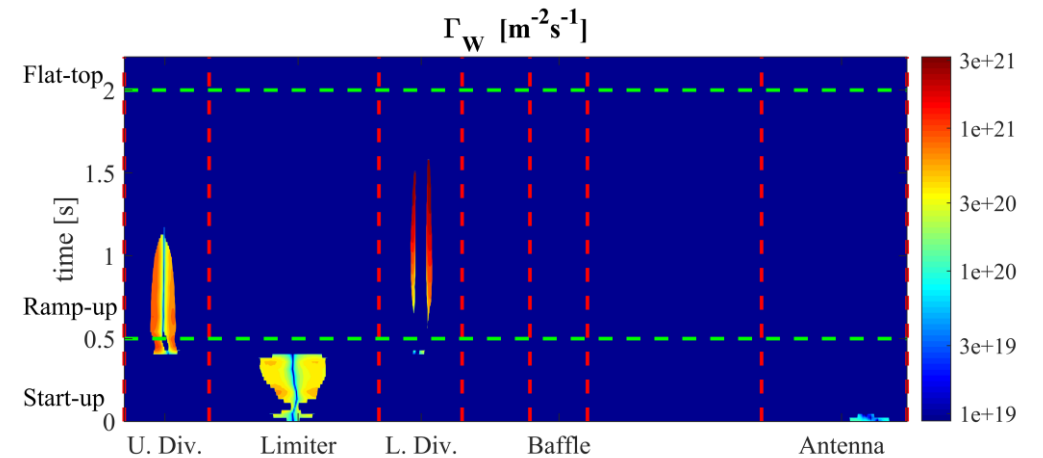
→ E_{impact} = energy to release a W atom in a D-W head collision

$$E_{impact} = 2k_b T_i + Z 3k_b T_e$$

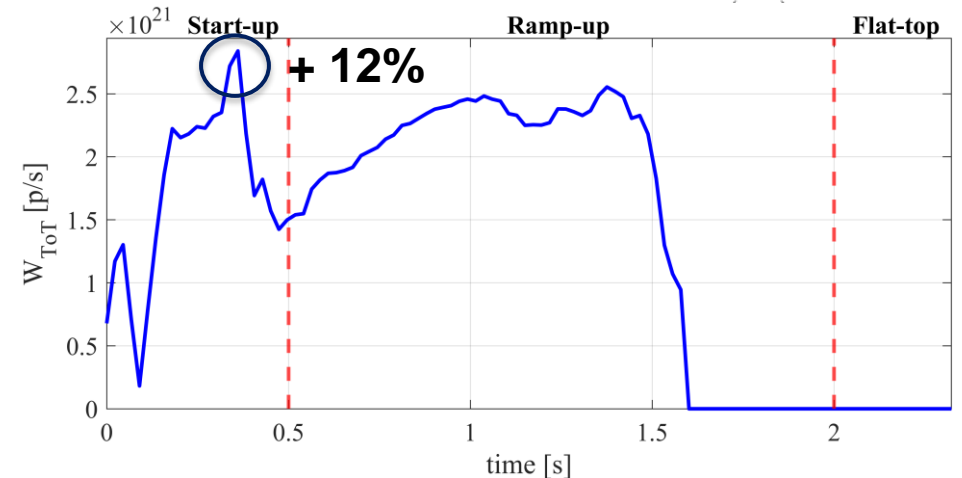
[P. C. Stangeby, The Plasma Boundary of Magnetic Fusion Devices, 2000]

[MS d'Abusco *et al.* N. Fus. 2022]

(a) $\Gamma_W(\mathbf{x}, t) = \mathcal{H}(E_{impact} > E_{th}) \Gamma_{D+}$ **Tungsten Influx**



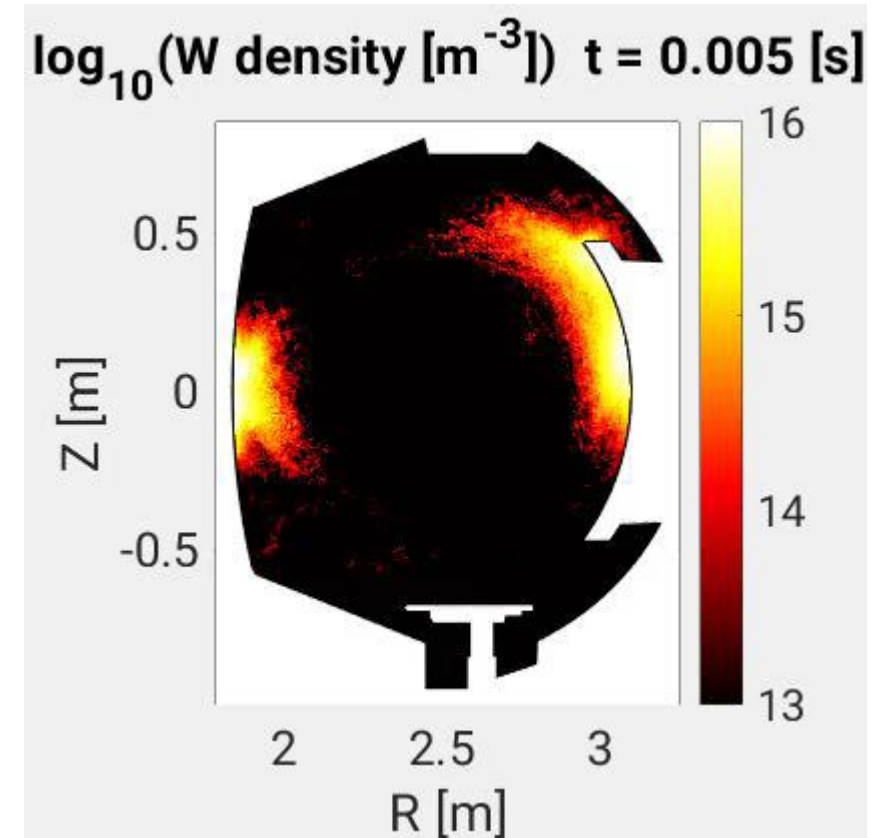
(b) $W_{ToT}(t) = \int_{\partial\Omega} \mathcal{H}(E_{impact} > E_{th}) \Gamma_{D+} ds$ **Tungsten Total Contamination**



WEST Shot #54487: Tungsten evolution using ERO

- SOLEDGE3X-HDG plasma backgrounds post processed by ERO 2.0 to compute the evolution of tungsten density
 - **Start-up phase:**
sputtering mainly concentrated on the high field left limiter and antenna and high core contamination
 - **X-point onset:**
sputtering mainly concentrated on the diverotr target (Upper and Lower)
- Good qualitative agreement with the crude cinematic model
 - Reproduction of the sputtering peak approximately at the same time $t = 0.4$ s

Tungsten Contamination



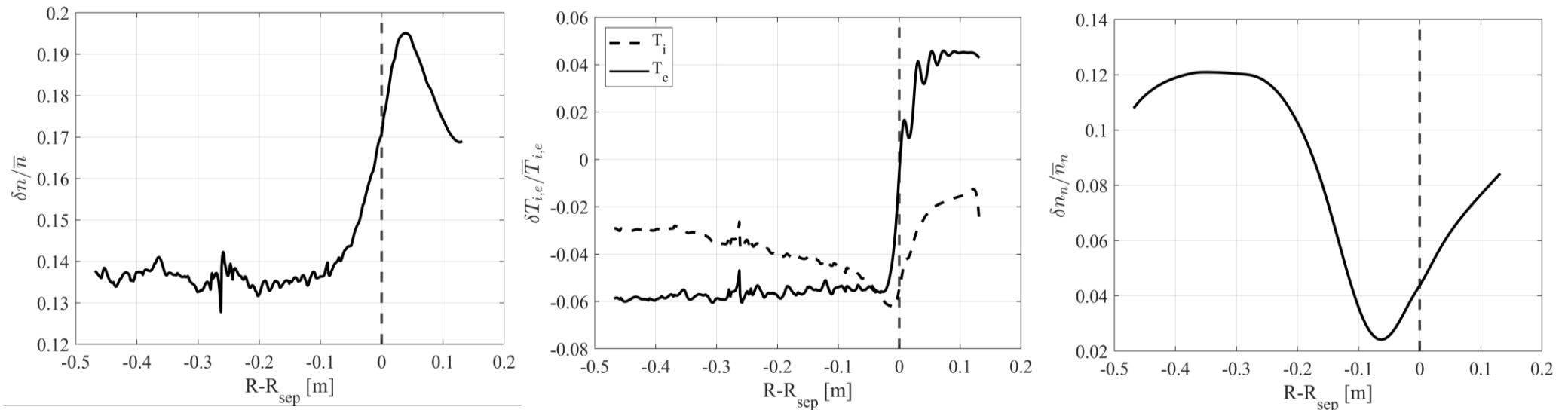
HDG #54487 background → ERO 2.0
[Montecarlo 3D code J. Romazanov et al., NME, 2019]

Outlines

- Mathematical and numerical model
- Verification and validation
- Core-edge coupling and sources
- Preliminary investigation of a detached plasma
- Full 2D transport simulations of an entire experimental discharge
- **Steady vs transient**

WEST Shot #54487: Steady vs transient

- Comparison with steady simulation performed at the flat top phase $t = 4.510$ s
→ higher value of plasma density in the unsteady computation than in the steady one



- The system doesn't reach the steady state over the time step of computation

[MS d'Abusco *et al.*
N. Fus. 2022]

$$\frac{1}{\tau_c} = \frac{\int_{\Omega} \partial_t n d\mathbf{x}}{\int_{\Omega} n d\mathbf{x}} \Big|_{t=4.51} = -3.15 \times 10^{-4} s^{-1} \Rightarrow \tau_c = 3 \times 10^4 s \text{ time scale to reach stationary state}$$

$$\frac{\partial N}{\partial t} = \frac{N}{\tau_c} + Q_{puff} \Rightarrow N(t) = Q_{puff} \tau (1 - e^{-t/\tau_c}) + N_0 e^{-t/\tau_c}$$

→ total number of particle relaxes to $Q_{puff} \times \tau_c$ over a time scale τ_c much greater than $dt = 0.02$ s

Steady vs transient in ERO

- **Calculation with transient phase:**

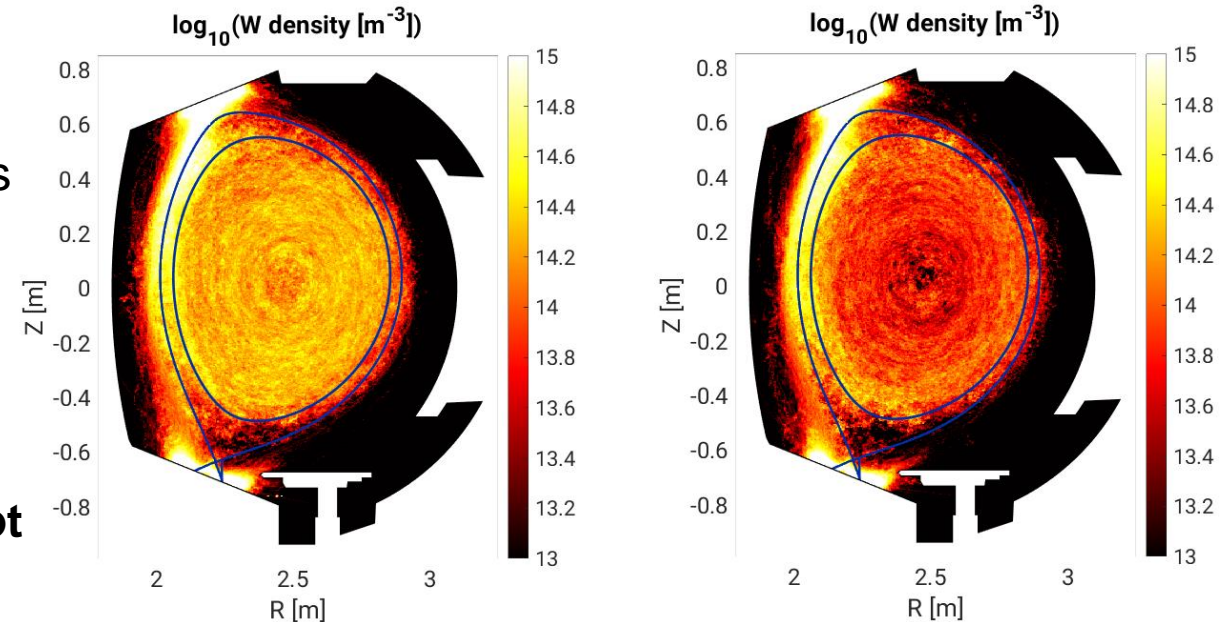
→ Evolution of the SE3X-HDG plasma backgrounds since the beginning of the discharge up to $t = 1.02$ s: **Left plot**

- **Steady:**

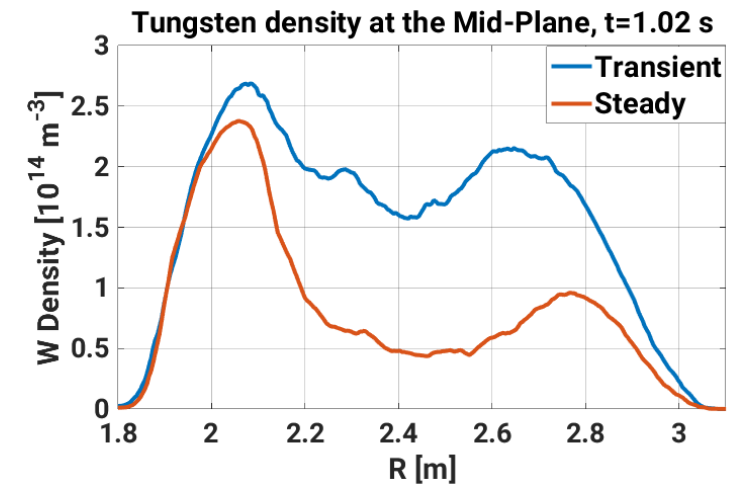
→ Fixed plasma background at $t = 1.02$ s: **Right plot**

- Higher core tungsten contamination when the transient phase is accounted

→ Tungsten density in the core 3 times greater for transient simulation vs steady case



Transient vs Steady at $t = 1.02$ s



Concluding remarks

- Core-edge transport fluid simulations have been performed in realistic tokamak geometry including transient phases: from start-up to shut-down
- Thanks to the new capabilities of the SOLEDGE3X-HDG: non-aligned grid + efficient time integration scheme + «self-consistent» sources

Physics highlights

- Heat fluxes estimation
 - Switch in the dominant power heat flux from electrons to ions in different phases of the discharge
 - Spreading in time of the power heat flux peaks along the divertor coordinates
- W sputtering and concentration:
 - Impact of the limiter-divertor transition: strong W contamination

This work confirms the interest on developing magnetic equilibrium free solver to support experimental data analysis and to target predictive capabilities in the future.

Future works and developments

- **Physics investigation:**

→ Investigation of **energy equipartition** problem by simple linear model: $\tau = \frac{T_i}{T_e}$

- **Two-short terms physical model improvements:**

→ Reduced model for cross-field transport: **k-epsilon**

→ Neutral sources: **Advanced fluid model** then **EIRENE** coupling

- **Numerical improvements increasing the DoF:**

→ **2D**

- Bigger size Tokamak simulations → **ITER** plasma volume \approx 30 times **WEST**
- **Multi-species** problem

→ **3D**

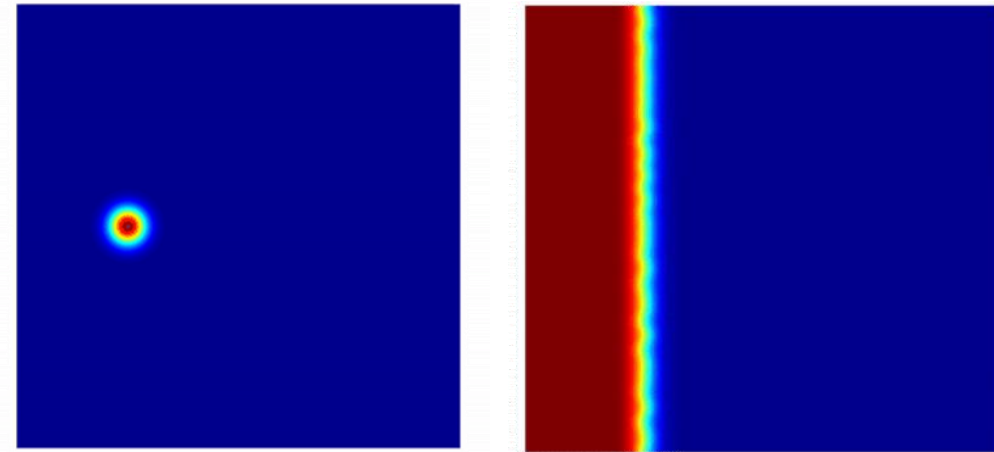
- Transport simulation in **non-axisymmetric** geometries or with **3D magnetic perturbation**
- Impact of **3D** plasma facing components on **transport proprieties** and **impurities**
- **3D turbulent** simulation at **ITER** scale

Preliminary results for future works

- 2D turbulent fluid model in SLAB geometry:
→ SLAB geometry

- First ITER real size simulation:
→ SOLPS-ITER like wall geometry
→ 2D non-isothermal model + fluid neutrals

Courtesy of
G. Giorgiani



MS. d'Abusco

